A bio-telemetric device for measurement of left ventricular pressure–volume loops using the admittance technique in conscious, ambulatory rats

2011 Physiol. Meas. 32 701

(http://iopscience.iop.org/0967-3334/32/6/007)

IOP PUBLISHING PHYSIOLOGICAL MEASUREMENT

Physiol. Meas. **32** (2011) 701–715 doi:10.1088/0967-3334/32/6/007

A bio-telemetric device for measurement of left ventricular pressure–volume loops using the admittance technique in conscious, ambulatory rats

Karthik Raghavan[1], Marc D Feldman[2], John E Porterfield[3], Erik R Larson[4], J Travis Jenkins[2], Daniel Escobedo[2], John A Pearce[4] and Jonathan W Valvano[4,5]

[1] Qualcomm, San Diego, CA 92121, USA
[2] Department of Medicine, University of Texas Health Sciences Center at San Antonio, San Antonio, TX 78229, USA
[3] Conductance Technologies, San Antonio, TX 78248, USA
[4] Department of Electrical and Computer Engineering, University of Texas at Austin, Austin, TX 78712, USA

E-mail: feldmanm@uthscsa.edu, jpearce@mail.utexas.edu and valvano@mail.utexas.edu

Received 20 July 2010, accepted for publication 4 April 2011
Published 23 May 2011
Online at stacks.iop.org/PM/32/701

Abstract

This paper presents the design, construction and testing of a device to measure pressure–volume loops in the left ventricle of conscious, ambulatory rats. Pressure is measured with a standard sensor, but volume is derived from data collected from a tetrapolar electrode catheter using a novel admittance technique. There are two main advantages of the admittance technique to measure volume. First, the contribution from the adjacent muscle can be instantaneously removed. Second, the admittance technique incorporates the nonlinear relationship between the electric field generated by the catheter and the blood volume. A low power instrument weighing 27 g was designed, which takes pressure–volume loops every 2 min and runs for 24 h. Pressure–volume data are transmitted wirelessly to a base station. The device was first validated on 13 rats with an acute preparation with 2D echocardiography used to measure true volume. From an accuracy standpoint, the admittance technique is superior to both the conductance technique calibrated with hypertonic saline injections, and calibrated with cuvettes. The device was then tested on six rats with 24 h chronic preparation. Stability of animal preparation and careful calibration are important factors affecting the success of the device.

Keywords: admittance, impedance, conductance, wireless, left ventricular pressure, left ventricular volume, rats, pressure volume loop

[5] Author to whom any correspondence should be addressed.

1. Introduction

Small mammals are a good choice for many experimental protocols because of their low cost and ease of handling. Pressure–volume (*P–V*) loops provide important physiological parameters for protocols involving myocardial function (Sagawa *et al* 1988, Franco *et al* 1998, 1999, Esposito *et al* 2000). The ability to measure left ventricular (LV) pressure and volume in real time during chronic preparations would be valuable to the physiologist and for drug discovery. This paper presents a prototype instrument to be used in conscious, ambulatory rats. There are three challenges in designing such a device. The first challenge is to minimize power, weight and size. The second challenge is to minimize the measurement error using a realistic understanding of electric field theory together with accurate calibrations. The third challenge is to design an apparatus that is comfortable for the animal. This initial instrument used a backpack configuration to house the circuitry and battery, and the *P–V* transducer was surgically placed in the left ventricle. The device presented in this paper is similar to the one presented by Uemura *et al* (2004), but employs the more accurate admittance technique. The conscious rat carried the backpack for the duration of the 24 h experiment. Future devices must be smaller and lighter so that the instrument itself does not affect animal physiology.

In this paper, we compare three techniques to determine end systolic volume (ESV), end diastolic volume (EDV) and stroke volume (SV). 2D echo is used as a reference for volume. We collected one set of data and analyzed it in three ways. The admittance data represents the results of our method.

(1) *Admittance*-derived volumes using Wei's equation (Wei *et al* 2005), dynamic α, and dynamic myocardial G_m (Porterfield *et al* 2009).

(2) *Conductance*-derived volumes using Baan's equation with a constant α, and a constant G_p derived from hypertonic saline calibration (Baan *et al* 1981). This is the data we collected but analyzed using one common calibration process.

(3) *Cuvette*-derived α and V_p used along with Baan's equation (Uemura *et al* 2004). This is the data we collected but analyzed using the other common calibration process.

2. Methods

2.1. Admittance technique

One contribution of this paper is the extension of the admittance technique first developed in mice (Feldman *et al* 2000, Kottam and Pearce 2004, Raghavan *et al* 2004, Wei *et al* 2005, Reyes *et al* 2006, Raghavan *et al* 2009, Porterfield *et al* 2009) to rats. A tetrapolar catheter is inserted into the left ventricle. A constant current at 20 kHz is delivered across electrodes 1 and 4, as shown in figure 1. Voltage is measured between electrodes 2 and 3. Complex admittance (magnitude and phase) is calculated from the current/voltage quotient. LV catheter admittance measurements involve contributions from the blood, the catheter itself and the myocardium. In order to estimate the contribution due to the blood accurately, it is necessary to estimate the myocardial and catheter contributions and eliminate these from the combined signal. When the tetrapolar catheter is placed in the left ventricle, the admittance measured is a combination of the contributions from the blood, the myocardium and the probe itself:

$$Y_{\text{meas}} = G_b + G_m + \mathrm{j}\omega C_m + \mathrm{j}\omega C_{\text{probe}}. \tag{1}$$

Let $Y_m = G_m + \mathrm{j}\omega C_m$ be the admittance contribution from the myocardium. A saline

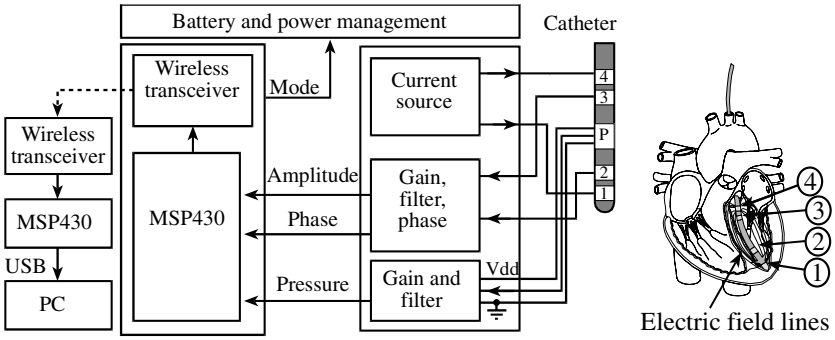

Figure 1. Block diagram of the backpack system, where the arrows show data/control flow. Four electrodes and a pressure sensor are placed in the left ventricle of a rat. A small 20 kHz current is applied across electrodes 1–4, and the resulting voltage difference across electrodes 2–3 is measured. Left ventricular volume is derived from measurements of admittance, so that pressure–volume loops can be chronically measured.

calibration is used to determine the contribution due to $j\omega\, C_{\text{probe}}$. The imaginary part is used to estimate muscle capacitance:

$$\text{j}\omega C_m = |Y_{\text{meas}}| \sin(\theta_{\text{meas}}) - \text{j}\omega C_{\text{probe}}, \tag{2}$$

where $|Y_{\text{meas}}|$ is the measured admittance magnitude and θ_{meas} is the measured phase angle. For any electric field spatial distribution, E, in a homogeneous medium:

$$G = \frac{I}{V} = \sigma \frac{\int\int E \bullet \text{d}A}{-\int E \bullet \text{d}l} = \sigma F \tag{3a}$$

$$C = \frac{Q}{V} = \varepsilon \frac{\int\int E \bullet \text{d}A}{-\int E \bullet \text{d}l} = \varepsilon F \tag{3b}$$

where I is the current (A), V is the potential (V), σ is the electrical conductivity (S m^{-1}), Q is the charge (C), ε is the electric permittivity (F m^{-1}), and F is the electric field form factor, or 'cell constant', common to both relations (m). The symmetry in the relationships of equations (3*a*) and (3*b*) leads to the familiar 'conductance–capacitance' analogy. The symmetry is also the feature that allows identification and elimination of the cardiac muscle from the combined admittance signal: if C_m is measured, then G_m can be calculated by a simple ratio, $G_m = C_m\, \sigma/\varepsilon$, where the σ/ε ratio is a property constant of the myocardial tissue (Raghavan *et al* 2009, Porterfield *et al* 2009). Putting these together, the blood conductance can be calculated:

$$G_b = |Y_{\text{meas}}| \cos(\theta_{\text{meas}}) - G_m. \tag{4}$$

Baan's equation (1981) assumes a linear relationship between volume and blood conductance. However, we feel the nonlinear Wei's equation more accurately describes the relationship between volume and blood conductance (Wei *et al* 2005, 2007, and Porterfield *et al* 2009):

$$V = \frac{1}{\alpha} \rho L^2 G_b \qquad \text{(Baans' equation)} \tag{5a}$$

$$V = \frac{1}{1 - G_b/\gamma} \rho L^2 G_b \qquad \text{(Wei's equation)} \tag{5b}$$

where γ is a calibration constant, ρ is the resistivity of blood, and L is the distance between electrodes 2 and 3 on the catheter. The γ-calibration occurs by operating the device *in vivo* with known SV or known EDV. The geometry correction factor, γ, is calculable from an independent measurement of the SV:

$$\gamma = \frac{-b \pm \sqrt{b^2 - 4ac}}{2a} \qquad \begin{array}{c} a = \mathrm{SV} - \rho L^2 (G_{b-\mathrm{ED}} - G_{b-\mathrm{ES}}) \\ b = -\mathrm{SV}\ (G_{b-\mathrm{ED}} + G_{b-\mathrm{ES}}) \\ c = \mathrm{SV}\ \cdot G_{b-\mathrm{ED}} \cdot G_{b-\mathrm{ES}} \end{array} \tag{6}$$

where ED refers to end diastole and ES refers to end systole. The SV must be measured at the same time by an independent method such as an aortic flow probe or echocardiography in order to force the measured SV to match the true SV. When calibrating with echocardiography, finding γ is easier because we know the EDV:

$$\gamma = \frac{G_{b-\mathrm{ED}}}{1 - \frac{\rho L^2 G_{b-\mathrm{ED}}}{\mathrm{EDV}}}. \tag{7}$$

2.2. Backpack design

In order to provide comfort for the conscious rat, an instrument was developed with three main constraints: low power (LP), small volume, and low weight. A small volume and low weight enable the rat to perform regular activities related to intake of food and water, and to freely roam in its cage while carrying the backpack. In addition to these constraints, the instrument should be accurate and stable. The goal was to operate for 24 h, wirelessly transmitting *P–V* data every 2 min.

Figure 1 is the data flow graph of the backpack instrument. A 3.7 V, 625 mAh Li-ion battery is used to power the circuit. The battery weighed 18.5 g, which is about 67% of the total weight of the system. The circuit is based on a single-supply design with the clock generator, phase detector chip, operational and differential amplifiers functioning on a single 3.6 V supply (using LP voltage regulators: LT1761ES5-SD). An analog virtual ground at 1.8 V was created with a precision reference chip (REF3318). All the components were chosen to minimize power while meeting the required voltage swings, bandwidth and slew-rate. To minimize volume, quad-package LP operational amplifiers (LM6134) were used, wherever possible. All resistors are precision metal–film resistors (1% tolerance) and all capacitors were ceramic capacitors (10% tolerance).

The backpack included a microcontroller board, an instrumentation board and the Li-ion battery. The instrumentation consisted of a LP 20 kHz sinusoid generator followed by a LP voltage-to-current converter. The 20 kHz sinusoidal generator used a combination of LP oscillator: LTC6906 and high-Q band pass filter at 20 kHz. This generated a 10 μA rms current, to the outer two electrodes of the catheter (electrodes 1 and 4). The voltage signal generated from the inner electrodes (electrodes 2 and 3) was then amplified using a LP instrumentation amplifier (INA331IDGK), followed by a gain and filtering stage. This was used to generate a dc signal corresponding to the admittance magnitude signal using a full wave rectification stage. In parallel, a phase detection chip (AD8302) was used to determine the phase difference between the original reference signal and the resulting output signal. A separate signal path was employed to process the pressure signal arising from the pressure transducer. The phase response of the pressure channel was designed to match the admittance channel, so that sampled volume and pressure data represent physiological parameters occurring at the same time in the cardiac cycle. The four-layer instrumentation printed circuit board was 2.74 in^2.

For the acute studies, the data was collected using Chart Software (AD Instruments, Bella Vista, NSW, Australia). For the chronic studies, the data was transmitted wirelessly to a laptop. The microcontroller board included an MSP430F2274 microcontroller with CC2500 2.4 GHz wireless transceiver (Texas Instruments, Dallas, TX). The MSP430F2274 microcontroller was an ultra-low power system drawing a maximum active current of 390 μA. In the standby mode, it draws a maximum current of 1.4 μA. The CC2500 transceiver was also low power with programmable data rates from 1.2 to 500 kbps drawing a typical current of 21.2 mA during sampling. The resulting magnitude, phase and pressure signals from the instrumentation were fed to the inputs of three 10 bit ADCs on the MSP430F2274 microcontroller. The low power, low bit-rate SimpliciTI^{TM} protocol was used to transmit the signals over a radiofrequency (RF) link to the other transceiver. This RF link requires less power than the Bluetooth device used by Uemura *et al* (2004). The receiver was placed approximately 2 m away connected to a laptop. Data were collected and stored on this laptop for post-processing analysis and display. The board power regulators were controlled by an enable signal (labeled Mode in figure 1). The microcontroller software applies power to the analog electronics during data acquisition, which is 12 s every 2 min. Power is disabled to the analog circuits and RF link for the remainder of the time. A soft but strong mechanical buffer surrounds the backpack to protect the circuit during times when the rat is active.

The instrumentation board along with the microcontroller board weighed about 9 g, which is less than 14 g instrument designed by Uemura *et al* (2004). With a 625 mAh Li-Ion battery the total weight was 27 g, slightly higher than the 26 g Uemura device. The system has two modes, 90% of the time it runs in standby mode, and 10% in active mode. In standby mode, the MPS430 is running in low power mode 3, the ADC, transmitter and analog electronics are off. The system draws about 22 mA in standby mode and 42 mA in active mode, resulting in an average current of 24 mA and allowing the system to run for over 24 h.

2.3. Calibration

The impedance magnitude was calibrated with four known precision resistors connected as the test load in place of the *P–V* catheter. The resistor was placed between electrodes 2 and 3 and electrode 1 was shorted to electrode 2 and similarly electrode 4 was shorted with electrode 3, creating a purely resistive load. The 1% metal-film resistors were chosen to represent the entire range of impedance magnitudes anticipated from a rat LV *P–V* experiment: 500 Ω to 2 kΩ. A linear relationship was obtained between the measured admittance magnitude and the true admittance.

To calibrate the phase detection chip, known parallel *R–C* load combinations were connected as the test load in place of the *P–V* catheter; the phase difference was calculated at a frequency of 20 kHz. A linear relationship was obtained between the phase difference and the *Phase* output voltage.

In order to eliminate the effects of the *P–V* catheter, the catheter was connected to the circuit and the electrodes were submerged into saline solutions of known conductivity: 1025 to 5690 μS cm^{-1}. Table 1 represents a typical saline calibration table.

σ is the true conductivity of the saline solution. $|Y|$ is the admittance magnitude, and ϕ is the phase, both measured with the backpack system. ReY is the real part of Y, and ImY is the imaginary component of Y. ImY is equal to the $j\omega C_{probe}$ term from equation (1). F is the electric field form factor (Re Y/σ) defined in equation (3*a*) (Raghavan *et al* 2009).

Table 1. Saline calibration.

σ (μS cm^{-1})	$\|Y\|$ (μS)	ϕ (deg)	Re Y (μS)	Im Y (μS)	F (m)
1025	617	18.0	587	191	0.005 73
1882	746	15.8	718	204	0.003 81
2860	1582	6.5	1572	180	0.005 50
3540	1639	6.1	1630	175	0.004 60
5690	2079	4.0	2074	145	0.003 65
				Avg	0.004 66

3. Animal studies

The main objective of the animal studies was to determine the viability of the admittance technique in obtaining telemetric LV P–V relations in chronic, untethered freely roaming, conscious rats. The animal experiments were divided into four groups. The first three groups were performed with rats on the surgical bench (acute studies) to demonstrate the accuracy of the admittance technique compared to the traditional conductance technique in $N = 17$ rats (Baan *et al* 1981, Gawne *et al* 1987, Lankford *et al* 1990, Georgakopoulos *et al* 1998, White *et al* 1998, Yang *et al* 2001, Georgakopoulos and Kass 2000, Uemura *et al* 2004). The fourth group was the telemetric 24 h chronic studies performed with the $N = 6$ rats roaming freely in the cage. For comparison with previously established techniques, volumes were also calculated using cuvette-based volume calibration. All $N = 23$ rats used for all the studies were of the WKY strain (white (albino) color). All experiments were approved by the Institutional Animal Care and Use Committee at the University of Texas Health Science Center in San Antonio.

3.1. Group 1: acute—myocardial conductivity and permittivity, and blood conductivity

This study involved the determination of myocardial electrical properties (σ and ε) using an epicardial surface probe (Raghavan *et al* 2009). This study was also used to determine the electrical conductivity of rat blood. Rats ($N = 4$) were anesthetized using an isoflurane container. The rats were then placed on the surgical bench, and anesthesia was maintained using 1% isoflurane delivered via a respirator (Harvard Rodent Ventilator Model 683, Harvard Apparatus, Holliston, MA) at a rate of 70 breaths min^{-1}. The chest was opened via median sternotomy. The epicardial surface probe was placed on the LV epicardium of the intact beating heart using a micro-manipulator (Raghavan *et al* 2009). The admittance magnitude and phase were measured using the backpack instrumentation and recorded using Chart Software. After the myocardial property measurements, 4 mL of blood was extracted from the LV using a 23-gauge needle and placed into a vial. This vial was placed in a 37 °C water bath (Precision water bath, Thermo Fisher Scientific, Waltham, MA). Using the epicardial surface probe, admittance measurements were performed to determine the electrical conductivity of blood.

3.2. Group 2: acute closed chest (CC)—comparison of admittance to traditional conductance techniques

This study was performed to compare admittance-derived volume with traditional conductance (magnitude–only) derived volume in a closed chest (CC) preparation. For the traditional method, the myocardial contribution was estimated in two ways: using a hypertonic saline

bolus administration and using cuvette calibration (Baan *et al* 1981, Gawne *et al* 1987, Lankford *et al* 1990, Georgakopoulos *et al* 1998, White *et al* 1998, Yang *et al* 2001, Georgakopoulos and Kass 2000, Uemura *et al* 2004). Rats ($N = 7$) were anesthetized using an isoflurane container. After the rats were placed on a 37 °C temperature-controlled surgical bench, the anesthesia was maintained using 1% isoflurane delivered via a respirator at a rate of 70 breaths min^{-1} with 100% O_2. A small neck incision was made to expose the jugular vein. An IV catheter was placed into the jugular vein for later administration of IV bolus hypertonic saline. A similar incision was made to expose the right carotid artery. The *P–V* catheter was guided into the LV via the carotid artery. The chest was shaved and gel (Parker Aquasonic 100 Ultrasound Transmission Gel, Parker Laboratories Inc., Fairfield, NJ) was applied on the chest. The 2D echocardiogram (Philips HDI 5000CV) probe was placed on the top of the beating heart.

The admittance magnitude and phase were measured using the backpack instrumentation and recorded using the Chart Software. LV Pressure was also measured in parallel using a Scisense Pressure Control Unit, FP891B (Scisense Inc., London, ON, Canada). A 2D echocardiogram was performed through a closed chest (CC Echo). After the CC Echo, hypertonic saline boluses were injected via the incision made on the jugular vein. A total of three 0.2 mL boluses of 3% hypertonic saline (3 g of NaCl in 100 mL of solution) were administered in sequence. During each bolus administration, the impedance magnitude was measured (at 20 kHz) using the backpack instrument and recorded using Chart software.

An alternative approach to calibrate the traditional conductance measurements was to drill holes of the size of an average rat LV in a Plexiglas block and to determine the output voltage to a true volume relationship. The holes were deep enough so that the entire catheter could be submerged. Seven different holes were drilled. The diameters of the holes ranged from 2.79 to 10.67 mm. These holes were filled with saline solutions (two different experimental solutions: 0.4 and 0.5 S m^{-1}). The catheter was submerged in each of these holes for each of the solutions (a total of $7 \times 3 = 21$ measurements). Impedance magnitude was measured to determine the volume calibration constant (α).

3.3. Group 3: acute open chest (OC) SV studies: comparison of admittance to 2D echo

To determine the impact of air surrounding the heart and confining the electric field on the admittance technique, the device was also tested in an acute open chest (OC) model. Rats ($N = 6$) were anesthetized using an isoflurane container. The *P–V* catheter was guided into the LV via the carotid artery. The chest was opened via a median sternotomy. An acoustic offset was used to obtain 2D echo images of the LV with the heart exposed (OC Echo). The OC echo image was used to determine LV EDV, LV ESV, and SV. An ultrasonic flow probe (Transonic flow probe, Serial # 2.5PSB1154, Transonic Systems Inc., Ithaca, NY) was placed around the ascending aorta. Using a flowmeter (TS420: Transit time perivascular flowmeter, Transonic Systems Inc., Ithaca, NY), the aortic blood flow was measured and recorded using Chart.

3.4. Group 4: chronic—telemetric rat studies

24 h chronic studies were performed on $N = 6$ rats. The rats were anesthetized using an isoflurane container. After the rats were placed on the surgical temperature-controlled bench, the anesthesia was maintained using 1% isoflurane delivered via a respirator at a rate of 70 breaths min^{-1} with 100% O_2. A 2D echocardiogram was performed through a closed chest (CC Echo). This served as the baseline starting reference for the LV SV. A small incision

Table 2. Myocardial and blood electrical properties: results summary.

Rat	σ_b(S m^{-1})	σ_m(S m^{-1})	ε_r
1	0.525	0.184	16 670
2	0.581	0.164	17 578
3	0.563	0.210	12 538
4	0.558	0.190	13 530
Mean	0.557	0.187	15 079
Standard deviation	0.023	0.019	2424

was made on the back of the rat, and the *P–V* catheter was passed along this tract. The rat was turned to a supine position and the *P–V* catheter was passed to the midline of the neck. The carotid artery was exposed and the *P–V* catheter was guided into the LV. A tie was made close to the neck incision. The rat was turned to lie face down. A jacket was placed around the shoulders of the rat (Guinea-pig jacket, Catalog # 620 069, Harvard Apparatus, Holliston, MA). The complete backpack (with the lithium ion cell and two circuit boards) was placed in the mechanical buffer and placed between the rat's body and the jacket. The jacket was then closed and umbilical tape was used to secure the backpack inside the jacket. The rat was placed in a cage for anesthesia recovery. Admittance magnitude, phase and pressure were measured, for 12 s every 2 min, using the backpack. Data were transmitted wirelessly to the laptop for 24 h recording. The rat was monitored during the entire time with periodic water and feeding. After 24 h had elapsed, the rats were placed on the temperature-controlled surgical bench, the anesthesia was maintained using 1% isoflurane delivered via a respirator at a rate of 70 breaths min^{-1} with 100% O_2. The chest was opened via median sternotomy. 4 mL of blood was extracted from the LV using a 23-gauge needle and placed into a vial. This vial was placed in a 37 °C water bath. Using the surface probe, admittance measurements were made to estimate the electrical conductivity of blood. At the conclusion of all rat experiments, the LV was exposed to verify proper placement of the *P–V* catheter.

4. Results

4.1. Group 1: acute—myocardial conductivity and permittivity, and blood conductivity

All measurements in this paper were performed using the backpack instrument. Measuring the electrical conductivity of blood (σ_b) is a simple procedure, because the blood does not produce phase shifts, so the phase responses can be neglected (Raghavan *et al* 2009). Table 2 summarizes the results of the estimates of the myocardial and blood electrical properties from $N = 4$ rats.

4.2. Group 2: acute CC studies—comparison of admittance to traditional conductance techniques

The seven male rats in the acute CC studies had weights ranging from 232 to 278 g with a mean weight of 254 g (standard deviation = 31 g). The hypertonic saline injection technique is one method for estimating the myocardial parallel conductance (G_p). This technique assumes that the parallel conductance is a constant and does not change during the heart cycle (Baan *et al* 1981, Georgakopoulos *et al* 1998). This technique involves introduction of hypertonic saline bolus into the circulatory system and measuring the end-systolic conductance (G_{ES})

and end-diastolic conductance (G_{ED}). As the saline progresses through the system, the blood conductance increases. These points are then plotted against each other on an G_{ES} versus G_{ED} plane and extrapolated to the line of identity, where, it is assumed that when $G_{ES} = G_{ED}$, the resulting conductance is the parallel conductance.

The data labeled 'conductance' was calibrated using injections of 3% hypertonic saline. The averages of one to four injections were used to determine G_p for each rat. This G_p was then used in Baan's equation to estimate the LV volume. G_p varied from 455 to 999 μS across the seven rats. The calibration factor α is obtained using the ratio of the derived SV (using Baan's equation with a first pass assumption of $\alpha = 1$) to the actual SV (obtained using 2D echo) (Baan *et al* 1981). Once α and G_p are obtained, volume is re-estimated using Baan's equation. This allows the results measured by admittance to be compared to the volumes derived from Baan's technique with hypertonic saline calibration.

Another popular technique involves the 'cuvette' method to map conductance to volume. Cuvette calibration is fit to Baan's equation (Baan *et al* 1981):

$$V = \frac{\rho L^2}{\alpha}(G - Gp) \quad \text{or} \quad V = \frac{\rho L^2}{\alpha}G - Vp \tag{8}$$

where the parallel volume V_p is defined as $G_p \rho L^2/\alpha$. The blood volume in Baan's equation is assumed to be the cuvette volume. The slope of the $\rho L^2 G$ versus volume curve is a measure of α. In the cuvette experiment, because the cuvettes are holes drilled into Plexiglas, one would have expected the parallel conductance G_p (and parallel volume V_p) to be 0. Calibration results show the measured $G_p \rho L^2$ is linearly related to the cuvette volume ($r^2 > 0.97$). The calibration data has a positive offset, and this offset is included as the calibration constant V_p in equation (8). Two different saline conductivity solutions were chosen (0.4 S m^{-1} and 0.5 S m^{-1}). The final α and V_p was the average of the two estimates. Using equation (8), α was estimated to be 0.394 and V_p was estimated at 218 μL.

The analyses are based on data collected during four sequential P–V loops. The admittance data were collected with our device. Conductance and cuvette data were derived from other commonly used calibration methods. Table 3 is a summary of the 2D echo EDV, ESV, SV and ejection fraction (EF) mean estimates and a comparison of this versus admittance, conductance and cuvette-based mean volume estimations. Bland–Altman plots are shown in figure 2 comparing admittance, conductance, and cuvette to the 2D echo data. Solid lines represent means, and dashed lines represent the 95% confidence intervals. The average error for admittance is 32.5 $\pm$ 40.1 μL. The average error for conductance is 472 $\pm$ 419 μL. The average error for cuvette is 126 $\pm$ 126 μL. The admittance technique has less error than SV-calibrated conductance ($P < 0.001$ in Student's t-test). Similarly, the admittance technique has less error than cuvette-calibrated conductance ($P < 0.02$).

4.3. Group 3: acute open chest (OC) studies: comparison of admittance to 2D echo

Similar to the CC studies, the admittance-derived volume was compared to 2D echo. The Bland–Altman plot for $N = 6$ rats is similar to the closed chest admittance studies, and consistent with the electric field not extending beyond the LV myocardium, as shown in figure 2(d).

4.4. Group 4: chronic—telemetric rat studies

Table 4 is a summary of the details of the rats used in the chronic studies ($N = 6$ rats). The body weights shown are at the start of the experiment and at the end of the 24 h experiment. A paired Student's t-test shows a significant drop in weight with $p < 0.01$. Figure 3 shows

Table 3. Closed chest (CC) comparison of 2D echo, admittance, conductance, and cuvette derived mean volumes.

	Echo CC				Admittance CC			Conductance CC			Cuvette CC		
Rat	EDV (μL)	ESV (μL)	SV (μL)	EF (%)	EDV (μL)	ESV (μL)	EF (%)	EDV (μL)	ESV (μL)	EF (%)	EDV (μL)	ESV (μL)	EF (%)
1	423	63	360	85	391	31	92	553	193	65	207	78	62
2	185	36	149	81	181	32	82	1510	1361	10	301	268	11
3	209	37	172	82	242	70	71	950	778	18	315	263	16
4	282	63	219	78	301	82	73	523	304	41	442	297	33
5	196	40	156	80	274	118	57	630	474	25	342	248	27
6	149	30	118	80	235	117	50	227	109	52	383	229	40
7	254	46	208	82	301	93	69	611	403	34	251	146	42

Table 4. Measurements before and after the chronic study, $N = 6$.

Rat	Sex	Weight 0 h (g)	Weight 24 h (g)	Weight loss (%)	HW (mg)	LVW (mg)	EDV 0 h (μL)	EDV 24 h (μL)	EDV change (%)
1	M	201	180	10.4	692	480	215	107	−50
2	M	208	197	5.3	645	477	174	125	−28
3	M	229	210	8.3	711	525	206	91	−56
4	M	247	225	8.9	795	615	144	207	+44
5	M	295	279	5.4	882	660	161	104	−35
6	M	307	287	6.5	912	700	216	153	−29
Mean		248	230	7.5	773	576	186	131	−26
Standard deviation.		44	44	2.1	108	96	31	43	36

the raw pressure and admittance data for the chronic study. Regression lines were found for pressure and admittance versus time. The null hypothesis is 'the pressure was constant throughout the experiment'. Calculating the *t*-score for the slope of the regression, only rat 4 showed a nonzero pressure slope with $p < 0.01$. Performing a similar trend analysis on the admittance data showed that all rats had a nonzero slope in Mag$|Y|$ with $p < 0.01$. The initial echo EDV was used to calibrate Wei's equation, equations (5*b*) and (7), determining γ after the probe was inserted into the LV. Figure 4 shows calibrated *P–V* loops for a typical rat at four different times. These *P–V* loops show a steady drop in volume.

5. Discussion

5.1. Applications

Scientists desire to perform chronic conscious studies on untethered rats to understand physiology and for new drug development. The classic method to assess the hemodynamic phenotype is through LV pressure–volume analysis. However, determining absolute and instantaneous volume in the conscious rat LV has been plagued by its small size and rapid heart rate. Traditional imaging technologies, such as MRI, are limited to providing the time-averaged overall structure. MRI is not capable of providing an instantaneously measured

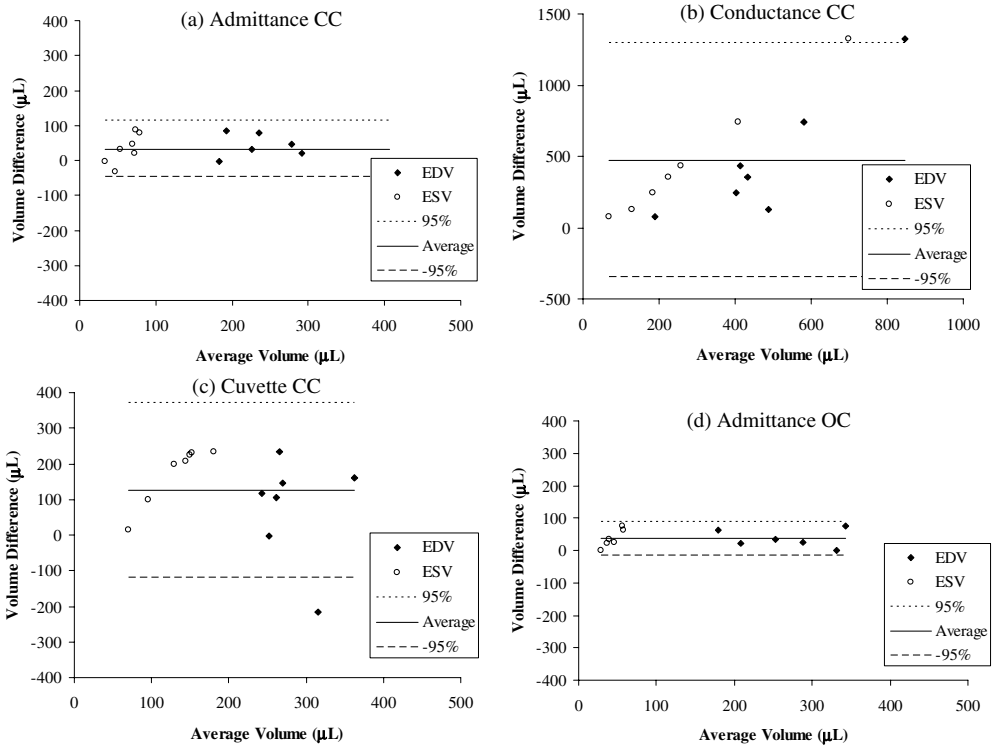

Figure 2. Closed chest (CC) Bland–Altman plots for $N = 7$ rats; open chest (OC) Bland–Altman plots for $N = 6$ rats. Our admittance method is experimentally verified in both closed (a) and OC (d) preparations. Two other commonly used calibration techniques were also evaluated: volume measured with conductance calibrated with hypertonic saline injections (b) and volume measured with cuvette calibration (c).

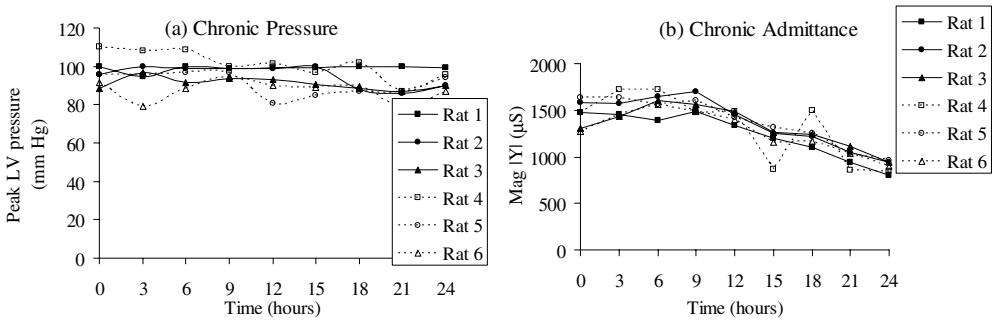

Figure 3. Six rats were instrumented with the backpack system and data was collected wirelessly for 24 h. 5 of 6 rats were p = NS for nonzero pressure slope. All rats were $p < 0.01$ for nonzero Mag$|Y|$ slope.

volume or derived physiologic function of the conscious rat heart. 2D echocardiography can sample volume overtime but requires sedation and can only measure load dependent measures of ventricular function such as fractional shortening and EF. Measurements of both pressure

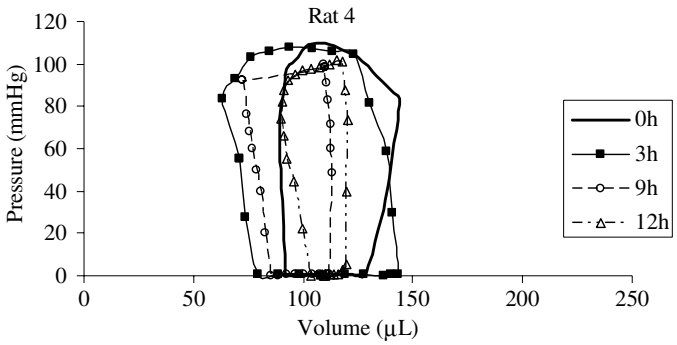

Figure 4. A rat was instrumented with the backpack system and data was collected wirelessly. The system allows pressure–volume loops to be measured.

and volume in a chronic conscious preparation would be a valuable tool to the research scientist.

5.2. Volume accuracy

Table 3 and figure 2 show the admittance-derived volumes using Wei's equation, dynamic α, and dynamic myocardial G_m is more accurate than conductance with hypertonic saline calibration or cuvette calibration. These results are consistent with the results obtained in mice (Raghavan *et al* 2009). Cuvette calibration continues to be a popular technique because of its simplicity (Ikonomidis *et al* 2005, Pacher *et al* 2005, Costandi *et al* 2006, Bergman *et al* 2007, Yue *et al* 2007). However, the results in this paper show improved accuracy can be obtained by using the admittance technique.

5.3. Admittance calibration

All conductance or admittance-based techniques rely on accurate knowledge of blood resistivity. The admittance technique also requires a calibration for the σ/ε ratio in cardiac muscle. The admittance technique requires a third calibration of either SV or EDV as measured by a flowprobe or echo device to obtain the γ constant in Wei's equation. The ESV measurements for all techniques will have large percentage errors because the volumes themselves are small. It is because of the large errors in ESV, we did not attempt to calibrate using ESV. There is a complex behavior occurring at the electrode–blood interface. Furthermore, the electric field shapes are complex and vary throughout the cardiac cycle. An advantage of the *in vivo* echo calibration over the *in vitro* cuvette calibration is that *in vivo* calibration incorporates the complexities of the probe-tissue system as they exist in this particular animal on this particular day.

5.4. Pressure–volume synchronization

A critical parameter for a *P–V* measurement is the relative timing between pressure and volume data. Both the volume and pressure channels have phase responses. Both filters exhibit a group delay, which may be interpreted as a time delay between the input wave and the digital samples. For example, a simple passive 100 Hz LPF will have a group delay of 1.6 ms for signals much less than 100 Hz. These delays may not be significant for large animals, but in

small rodents with fast heart rates it is important to design and calibrate the system such that pressure and volume channels are synchronized in time.

5.5. Catheter positioning

From a surgical perspective, one needs to see the *P–V* (or pressure-admittance) loops plotted in real time during the insertion of the catheter. Although centering the catheter in the middle of the ventricle is less critical for the admittance technique than for the conductance techniques (Raghavan *et al* 2009), it is still important to position the catheter so that physiologic shapes are observed in the *P–V* loops.

5.6. Backpack weight

Although all six rats survived the 24 h experiment, it is clear the backpack was too heavy. The 7.5% loss in body weight was a sign of dehydration and distress. All six rats showed a steady drop in admittance-derived EDV and consistent with the loss of body weight. In order to study the chronic behavior of the instrument, it will be important in the future to create a physiologically stable animal preparation.

5.7. Uemura device

In many ways this device is similar to the one designed by Uemura *et al* (2004). The sizes and weights are similar. Our device weighs 27 g, and the Uemura device weighs 26 g. Both devices are battery operated and have wireless links, so the conscious rats can freely roam above their cage. The Uemura device uses Bluetooth, and our device uses the SimpliciTI™ protocol. Both devices use a tetrapolar catheter placed in the LV (see figure 1) and measure instantaneous blood volume from electrical properties. Both devices also include a pressure sensor also positioned in the LV. Both devices employ a sinusoidal current source, analog signal processing, an ADC, and a microcontroller. Both devices use measurements taken in the ventricle to subtract parallel conductance (G_m), without the need for saline injections. The Uemura device used dual frequency, whereas our device uses the imaginary component of the admittance to remove the unwanted component in the signal caused by the electrical currents passing through the adjacent cardiac muscle. Wei *et al* (2007), Porterfield *et al* (2009) have shown that the parallel conductance varies throughout the cardiac cycle. The dual frequency technique assumes a constant value for parallel conductance, whereas the admittance technique calculates a separate G_m for each point in the cardiac cycle. Hence, when removing parallel conductance our device is superior to the Uemura device. In terms of accuracy, the Uemura device uses cuvette calibration. Although the cuvette calibration is simple to understand and simple to perform, the rat data in this paper and the mouse data in Porterfield *et al* (2009) show the admittance technique to be more accurate than the conductance calibrated with cuvettes.

6. Conclusions

The results in this paper demonstrate that it is possible to monitor pressure and volume in conscious, ambulatory rats. We conclude that for both open and closed-chest rats, admittance (dynamic G_p) and Wei's equation (dynamic α) provide more accurate volumes than traditional conductance. A 27 g backpack was designed and built capable of transmitting 12 s of real time *P–V* data every 2 min for 24 h. The device was calibrated with 2D echo and validated in

rats. The next step will be to reduce the size, weight and power so that longer measurement times can be achieved.

Acknowledgments

The authors would like to thank Rodolfo J Treviño from The University Health Sciences Center at San Antonio (UTHSCSA), San Antonio, TX, for his help with the murine experiments. This work was supported in part by the National Institute of Health under Grant R21 HL079926 and a VA Merit Grant (MDF). Catheters were supplied by Scisense Inc., London, Ontario, Canada.

References

Baan J, Jong T T, Kerkhof P L, Moene R J, van Dijk A D, Van Der Velde E T and Koops J 1981 Continuous stroke volume and cardiac output from intraventricular dimensions obtained with impedance catheter *Cardiovasc. Res.* **15** 328–34

Bergman M R, Teerlink J R, Mahimkar R, Li L, Zhu B, Nguyen A, Dahi S, Karliner J S and Lovett D H 2007 Cardiac matrix metalloproteinase-2 expression independently induces marked ventricular remodeling and systolic dysfunction *Am. J. Physiol. Heart Circ. Physiol.* **292** H1847–60

Costandi P N, Frank L R, McCulloch A D and Omens J H 2006 Role of diastolic properties in the transition to failure in a mouse model of the cardiac dilatation *Am. J. Physiol. Heart Circ. Physiol.* **291** H2971–9

Esposito G, Santana L F, Dilly K, Santos Cruz J D, Mao L, Lederer W J and Rockman H A 2000 Cellular and functional defects in a mouse model of heart failure *Am. J. Physiol. Heart Circ. Physiol.* **279** H3101–12

Feldman M D, Erikson J M, Mao Y, Korcarz C E, Lang R M and Freeman G L 2000 Validation of a mouse conductance system to determine LV volume: comparison to echocardiography and crystals *Am. J. Physiol. Heart Circ. Physiol.* **274** H1698–707

Franco F, Dubois S, Peschock R M and Shohet R V 1998 Magnetic resonance imaging accurately estimates LV mass in a transgenic mouse model of cardiac hypertrophy *Am. J. Physiol. Heart Circ. Physiol.* **274** H679–83

Franco F, Thomas G D, Giror B, Bryant D, Bullock M C, Chwialkowski M C, Victor R G and Peschock R M 1999 Magnetic resonance imaging and invasive evaluation of development of heart failure in transgenic mice with myocardial expression of tumor necrosis factor-α *Circulation* **99** 449–54

Gawne T J, Gray K S and Goldstein R E 1987 Estimated left ventricular offset volume using dual-frequency conductance technology *J. Appl. Physiol.* **63** 872–6

Georgakopoulos D and Kass D A 2000 Estimation of parallel conductance by dual-frequency conductance catheter in mice *Am. J. Physiol. Heart Circ. Physiol.* **279** H443–50

Georgakopoulos D, Mitzner W A, Chen C H, Byrne B J, Millar H D, Hare J M and Kass D A 1998 *In vivo* murine left ventricular pressure–volume relations by miniaturized conductance micromanometry *Am. J. Physiol. Heart Circ. Physiol.* **274** H1416–22

Ikonomidis J S, Hendrick J W, Parkhurst A M, Herron A R, Escobar P G, Dowdy P B, Stroud R E, Hapke E, Zile M R and Spinale F G 2005 Accelerated LV remodeling after myocardial infarction in TIMP-1-deficient mice: effects of exogenous MMP inhibition *Am. J. Physiol. Heart Circ. Physiol.* **288** H149–58

Kottam A and Pearce J 2004 Electric field penetration depth of myocardial surface catheters and the measurement of myocardial resistivity *Biomed. Sci. Instrum.* **40** 155–60

Lankford E B, Kass D A, Maughan W L and Shoukas A A 1990 Does volume catheter parallel conductance vary during a cardiac cycle? *Am. J. Physiol. Heart Circ. Physiol.* **258** H1933–42

Pacher P, Bátkai S, Osei-Hyiaman D, Offertáler L, Liu J, Harvey-White J, Brassai A, Járai Z, Cravatt B F and Kunos G 2005 Hemodynamic profile, responsiveness to anandamide, and baroreflex sensitivity of mice lacking fatty acid amide hydrolase *Am. J. Physiol. Heart Circ. Physiol.* **289** H533–41

Porterfield J, Kottam A, Raghavan K, Escobedo D, Jenkins J, Trevino R, Valvano J W, Pearce J A and Feldman M D 2009 Dynamic correction for parallel conductance, Gp, and gain factor, α, in invasive murine left ventricular volume measurements *J. Appl. Physiol.* **107** 1693–703

Raghavan K, Porterfield J, Kottam A, Feldman M D, Escobedo D, Valvano J W and Pearce J A 2009 Electrical conductivity and permittivity of murine myocardium *IEEE Trans. Biomed. Eng.* **56** 2044–53

Raghavan K, Wei C L, Kottam A, Altman D G, Fernandez D J, Reyes M, Valvano J W, Feldman M D and Pearce J A 2004 Design of instrumentation and data-acquisition system for complex admittance measurement *Biomed. Sci. Instrum.* **40** 453–7

Reyes M *et al* 2006 Impact of physiologic variables and genetic background on myocardial frequency-resistivity relations in the intact beating murine heart *Am. J. Physiol. Heart Circ. Physiol.* **291** H1659–69

Sagawa K, Maughan W L, Suga H and Sunagawa K 1988 *Cardiac Contraction and the Pressure–Volume Relationship* (New York: Oxford University Press)

Uemura K, Kawada T, Sugimachi M, Zheng C, Kashihara K, Sato T and Sunagawa K 2004 A self-calibrating telemetry system for measurement of ventricular pressure–volume relations in conscious, freely moving rats *Am. J. Physiol. Heart Circ. Physiol.* **287** H2906–13

Wei C L, Valvano J W, Feldman M D, Nahrendorf M, Peshock R and Pearce J A 2007 Volume catheter parallel conductance varies between end-systole and end-diastole *IEEE Trans. Biomed. Eng.* **54** 1480–9

Wei C L, Valvano J W, Feldman M D and Pearce J A 2005 Nonlinear conductance–volume relationship for murine conductance catheter measurement system *IEEE Trans. Biomed. Eng.* **52** 1654–61

White P A, Brookes C I, Ravn H B, Stenbøg E E, Christensen T D, Chaturvedi R R, Sorensen K, Hjortdal V E and Redington A N 1998 The effect of changing excitation frequency on parallel conductance in different sized hearts *Cardiovasc. Res.* **38** 668–75

Yang B, Beischel J, Larson D F, Kelley R, Shi J and Watson R R 2001 Validation of conductance catheter system for quantification of murine pressure–volume loops *J. Invest. Surg.* **14** 341–55

Yue P *et al* 2007 Magnetic resonance imaging of progressive cardiomyopathic changes in the db/db mouse *Am. J. Physiol. Heart Circ. Physiol.* **292** H2106–18